

Generating Hard Ising Instances With Planted Solutions Using Post-Quantum Cryptographic Protocols

Salvatore Mandrà,^{1,2,*} Humberto Munoz-Bauza,^{1,2} Gianni Mossi,^{1,2} and Eleanor G. Rieffel²

¹*KBR, Inc., 601 Jefferson St., Houston, TX 77002, USA*

²*Quantum Artificial Intelligence Lab. (QuAIL), NASA Ames Research Center, Moffett Field, CA 94035, USA*

In this paper we present a novel method to generate hard instances with planted solutions based on the public-private McEliece post-quantum cryptographic protocol. Unlike other planting methods rooted in the infinite-size statistical analysis, our cryptographic protocol generates instances which are *all* hard (in cryptographic terms), with the hardness tuned by the size of the private key, and with a guaranteed unique ground state. More importantly, because of the private-public key protocol, planted solutions cannot be easily recovered by a direct inspection of the planted instances without the knowledge of the private key used to generate them, therefore making our protocol suitable to test and evaluate quantum devices without the risk of “backdoors” being exploited.

I. INTRODUCTION

With the advent of more competitive (either quantum [1–3], quantum inspired [4–6] or post-Von Neumann [7–10]) technologies for the optimization of classical cost functions, it is becoming of utmost importance to identify classes of instances which are well suited to transversally benchmark such devices. One of the major challenges in designing planted problems is the generation of instances which are hard to optimize: indeed, planting a desired solution may affect the energy landscape of the instance, making it more convex and therefore easier to explore. Another important aspect that may affect the hardness of planted problems is the number of solutions: while it is guaranteed that the planted configuration *is* a solution, the planting protocol may introduce multiple solutions that would make the instance easier to solve.

In this work we introduce a way of generating Ising instances with one unique planted solution, whose hardness against optimization algorithms is derived from the robustness of the McEliece cryptographic protocol that is used to create them. The rest of the paper is organized as follows: in Section II we give an overview of the currently available planting methods for Ising Hamiltonians, in Section III we review linear codes, and the McEliece cryptographic protocol. Section IV shows how to generate hard instances of Ising Hamiltonians with planted solutions by recasting the McEliece protocol in Ising spin language, while Section V uses the machinery of statistical physics to illustrate why energy landscapes analogous to the ones exhibited by these hard instances should be difficult to explore for stochastic local search algorithms. In Section VI, we compare the performance of Parallel Tempering on the Ising formulation of the McEliece random instances against the best-known attack on the McEliece protocol.

II. OVERVIEW OF EXISTING PLANTING METHODS

For Constraint Satisfaction Problems (CSPs) like the graph coloring [11, 12] and the SAT problem [13], solutions can be planted by using the “quiet” planting technique [14–19]: constraints that satisfy the desired planted configuration are added until the required density of constraints is achieved. Similarly to random CSPs [20, 21], planted CSPs have different phase transitions by varying the density of constraints [16, 21–23]: while the “satisfiability” threshold is of course suppressed, phase transitions related to the hardness of the instances, such as the “freezing” transition [21], are preserved in planted instances. In particular, in frozen planted instances, solutions are all clustered into a single component which make the instance hard to optimize [24]. While the quiet planting can be used to quickly generate planted instances, properties like the hardness of the instances and the number of solutions are only true for the “typical” case and in the limit of a large number of variables, making the technique less valuable for small-scale and mid-scale benchmarks.

Similar to the quiet planting, the “patch” planting is a technique used to plant solutions for cost functions where not all the constraints must be satisfied at the same time [25–29]. More precisely, multiple subsystems with a known solution are “patched” together by properly applying hard constraints between subsystems. Solutions for each subsystem are found by either brute force or using other optimization techniques, and global solutions are obtained by patching together solutions from all the subsystems. The hardness of the patch planted instances is then tuned by increasing the size and the hardness of the subsystems [27]. Even if the patch planting technique can generate instances rather hard to optimize [28], one of the main downsides of the technique is that a direct inspection of the instances may easily reveal the solution. A random permutation of the variable indexes could mitigate the problem, but the use of cluster techniques [6] or the knowledge of the pre-permutation layout may still be used to identify each subsystem.

* salvatore.mandra@nasa.gov

Another common technique to plant solutions in combinatorial optimization problems consists in using exactly solvable models that present phase transitions. The simplest example is the problem of solving linear equations on the binary field (also called XORSAT [30]). More precisely, given a binary matrix \mathbf{A} of size $M \times N$, with M being the number of equations and N the number of variables, the XORSAT problem consists in finding the solution x such that $\mathbf{A}x = 0$, where the identity is modulo 2. If $M > N$, the fundamental theorem of linear algebra ensures that there are at least 2^{M-N} solutions. As for many other CSPs, XORSAT instances undergo different phase transitions by changing the density of constraints M/N , with the hardest instances being close to the satisfiability threshold [20]. While XORSAT instances are known to be hard to optimize using local heuristics, the simple knowledge of \mathbf{A} (regardless of any permutation of the variable indexes) is enough to find the set of solutions by using the Gaussian elimination.

A similar strategy is used in the generation of the *Wishart* instances [31]. In this case, real valued matrices $\mathbf{W} \in \mathbb{R}^{k \times N}$ are chosen such that $\mathbf{W}x^* = 0$ for the desired binary variable. Therefore, the corresponding binary cost function $H(x) = \frac{1}{2}x^T \mathbf{W}^T \mathbf{W}x = \frac{1}{2} \sum_{ij} J_{ij} x_i x_j$ is guaranteed to have x^* as a solution. The hardness of the Wishart instances is tuned by properly choosing the ratio $\alpha = k/N$, with an easy-hard-easy pattern by increasing α . Interestingly, the study of the Thouless-Anderson-Palmer (TAP) equations [32] applied to the Wishart problem shows the existence of a first order phase transition, making the Wishart instances hard to optimize for local heuristics. Moreover, unlike many other planting techniques, the Wishart instances are fully-connected and hard to optimize, even for a small number of variables. However, the hardness of the Wishart instances also depends on the digit precision of \mathbf{W} , making it less suitable for devices with a limited precision. Moreover, the number of solutions, which also may affect the hardness of the Wishart instances, cannot be determined except by an exhaustive enumeration and cannot be fixed in advance.

In [33], the fact that local heuristics have trouble optimizing frustrated loops is used to generate random instances with a known ground state, and hence the name Frustrated Cluster Loops (FCL). The ruggedness R of an FCL instance is how many loops a single variable is involved in, and it determines the hardness of the instances. Unfortunately, cluster methods easily identify these frustrated loops and therefore solve the FCL instances efficiently [34–36]. A variation of the FCL planting method has been used in [37] to generate hard instances. In this case, FCL instances are embedded on a Chimera graph with an embedding cost tuned by λ . The name Deceptive Cluster Loops (DCL) derives from the fact that for λ small enough, the ground state of DCL instances is mappable to the ground state of an equivalent 2D model, while for λ large to the ground state of a fully connected model. The hardness is then maximized at the transition

between the two limits. However, the ground state can only be determined at the extrema of λ .

Instead of taking the “shotgun” approach of generating spin-glass instances on a native graph until a sufficient number of hard instances are found, the hardness of the problem itself is treated as a cost function to optimize over the space of Ising Hamiltonians in [38], where they apply a Metropolis update rule on the Hamiltonian couplings to seek out harder instances. While the resulting instances are significantly harder, this approach requires an expensive quantification of the problem hardness by solving a new instance at every step. Furthermore, the ground state energies of the generated instances are not known in advance, and enforcing compatibility with a planted solution limits the available space of moves to generate novel and harder instances.

One of the first examples of the use of a private/public key protocol to generate hard instances can be found in [39]. More precisely, the authors of the paper use the subset sum problem [12], where a subset of a set of numbers $\Omega = \{\omega_1, \omega_2, \dots, \omega_N\}$ must be found such that their sum equals a given value c . The problem is known to be NP-Complete, and its quadratic binary cost function can be expressed as $H(x) = \sum_{i=1}^n (\omega_i x_i - c)^2$. However, the subset sum problem has a pseudo-polynomial time algorithm [40] which takes $\mathcal{O}(n\omega^*)$ memory, with ω^* being the largest value ω_i in the set. The Merkle-Hellman encryption algorithm works by using two sets of integers: the “private” key Ω , which is a super-increasing set of numbers, and a “public” key Ω' , which is defined as $\omega'_i = r\omega_i \bmod q$, with $q > \sum_i \omega_i$ and r being a random integer such that r and q are coprime. The values r and q are also kept secret. A message m_i of N bits is then encrypted as $c = \sum_i m_i \omega'_i$. On the one hand, without the knowledge of the private key, one must optimize the quadratic binary cost function $H(x) = (\omega'_i x_i - c)^2$ in order to find the encoded message. On the other hand, thanks to the fact that Ω is a set of super-increasing numbers and that the inverse of r modulo q can be efficiently found using the extended Euclidean algorithm, one can easily recover the binary message without the optimization of $H(x)$. The fact that the binary message m_i is recoverable guarantees that the ground state must be *unique*. Unfortunately, the use of super-increasing sequence of numbers makes the Merkle-Hellman protocol vulnerable to attacks [41] by just looking at the public key Ω' . Moreover, the complexity from the computational point of view depends on ω^* which sets the minimum digit precision for the set Ω . That is, exponentially hard integer partition instances require exponentially large ω_i , limiting the use of this protocol on devices with limited precision.

Recently, the integer factorization problem has been used to generate hard binary instances [42, 43]. More precisely, given two large prime numbers a and b of N -binary digits, the binary cost function is defined as $H(x, y) = \left[\left(\sum_{i=1}^N 2^i x_i \right) \left(\sum_{i=1}^N 2^i y_i \right) - c \right]^2$, with $c =$

ab. Instances based on factoring become exponentially hard by increasing the number of binary digits N . While no known classical algorithms are known to efficiently solve $H(x, y)$ without actually optimizing the binary cost function, factoring is vulnerable to quantum attacks via the Shor algorithm [44]. Moreover, the optimization of the binary cost function $H(x, y)$ requires an exponential precision, making such instances unsuitable for devices with limited precision.

III. BACKGROUND ON LINEAR CODES

To simplify the reading, for the rest of the paper it is assumed, unless otherwise specified, that all matrices and linear algebra operations take place over the finite field $\mathbb{F}_2 \equiv \mathbb{Z}/2\mathbb{Z}$, *i.e.* module 2 addition and multiplication over bits. Let us define the generator matrix $\mathbf{G} \in \mathbb{F}_2^{k \times N}$ of a linear code C , with $k \leq N$, and its check matrix $\mathbf{H} \in \mathbb{F}_2^{(N-k) \times n}$ such that $\mathbf{H}\mathbf{G}^T = 0$. A message $x \in \mathbb{F}_2^k$ can be then encoded as a string $y \in \mathbb{F}_2^N$, called the codeword, via

$$y \equiv x \mathbf{G}. \quad (1)$$

The code rate of C is defined as $R = k/N$, which is the average rate of useful information (the k -bit message) received per bit transmitted with the code (the N -bit codeword). Codes with smaller rates can incorporate more redundant bits which makes them resistant to random errors when transmitted across a noisy channel. The distance of C is defined as the minimum Hamming weight (the number of non-zero bits) among all the possible non-zero codewords, that is:

$$d \equiv \min_{x \in \mathbb{F}_2^k, x \neq 0} \|x \mathbf{G}\|, \quad (2)$$

where $\|\cdot\|$ indicate the Hamming weight. By the linearity of the code, the Hamming distance $\|y_1 - y_2\|$ between any two codewords y_1 and y_2 is at least d . Thus, a linear code of distance d can detect up to $d - 1$ errors and correct up to $(d - 1)/2$ errors. Indeed, let us define a vector ϵ with $t = |\epsilon|$ ones. The error would alter the encoded message as:

$$y' = x \mathbf{G} + \epsilon \quad (3)$$

Since $x \mathbf{G}\mathbf{H}^T = 0$ by construction, applying the parity check to y' one gets:

$$y' \mathbf{H}^T = \epsilon \mathbf{H}^T \equiv z. \quad (4)$$

where z is called the syndrome of the error. However, if $t < d$, ϵ cannot be a codeword of C and therefore $\epsilon \mathbf{H}^T \neq 0$, that is the code C can detect up to $d - 1$ errors. The three parameters N , k , and d are the most important characterization of linear codes, so we conventionally denote them by writing that C is an $[N, k, d]$ linear code.

An error can be instead corrected if, for a given syndrome $z = \epsilon \mathbf{H}^T$, it is possible to unequivocally identify ϵ . This is the case when two errors ϵ_1 and ϵ_2 produce two different syndromes. More precisely

$$\epsilon_1 \mathbf{H}^T \neq \epsilon_2 \mathbf{H}^T \Rightarrow (\epsilon_1 - \epsilon_2) \mathbf{H}^T \neq 0, \quad (5)$$

that is $\epsilon_1 - \epsilon_2$ is not a codeword of C . However, if ϵ_1 and ϵ_2 have respectively t_1 and t_2 errors, their sum cannot have more than $t_1 + t_2$ errors, implying that two syndromes can be distinguished only if the number of errors is smaller than $t \leq (d - 1)/2$.

A. McEliece Public/Private Key Protocol

In 1978, Robert McEliece discovered that linear codes C can be used as asymmetric encryption schemes [45]. While not getting much acceptance from the cryptographic community because of its large private/public key and being vulnerable to attacks using information-set decoding [46], the McEliece protocol has recently gained more traction as a “post-quantum” cryptographic protocol, as it is immune to the Shor’s algorithm [47]. At the time of writing, NIST has promoted the McEliece protocol to the phase 4 of its standardization [48].

In the McEliece protocol, the private key consists of a linear code C of distance d (with \mathbf{G} and \mathbf{H} being its generator matrix and check matrix respectively), a (random) permutation matrix $\mathbf{P} \in \mathbb{F}_2^{N \times N}$, and a (random) non-singular matrix $\mathbf{S} \in \mathbb{F}_2^{k \times k}$. On the other hand, the public key is defined as a new generator matrix $\mathbf{G}' = \mathbf{S}\mathbf{G}\mathbf{P}$ with distance d . Indeed, $\|x \mathbf{G}'\| = \|x \mathbf{S}\mathbf{G}\mathbf{P}\| = \|x \mathbf{S}\mathbf{G}\|$ since the Hamming weight is invariant by permutation, and

$$\min_{x \in \mathbb{F}_2^k, x \neq 0} \|x \mathbf{S}\mathbf{G}\| = \min_{y \in \mathbb{F}_2^k, y \neq 0} \|y \mathbf{G}\| = d, \quad (6)$$

where we used the fact that \mathbf{S} is non-singular and $y = x \mathbf{S}$. It is important to notice that it is hard to recover the original generator matrix \mathbf{G} from \mathbf{G}' without the knowledge of \mathbf{P} and \mathbf{S} . In the McEliece protocol, \mathbf{S} is used to “obfuscate” the original generator matrix \mathbf{G} by scrambling it. In the next Section, we will use a similar concept to create hard instances with a known and unique ground state.

The message encoding is then obtained by applying the public key \mathbf{G}' to an arbitrary message $q \in \mathbb{F}_2^k$ and randomly flipping a number $t = (d - 1)/2$ of bits, that is:

$$q' \equiv q \mathbf{G}' + \epsilon, \quad (7)$$

with $\|\epsilon\| = t$. If the private key is known, the message q can be recovered by observing that $\epsilon' = \epsilon \mathbf{P}^{-1}$ preserves the number of errors. Therefore the permuted encoded message $q' \mathbf{P}^{-1} = q \mathbf{S}\mathbf{G} + \epsilon'$ can be “corrected” using the parity check \mathbf{H} . Indeed

$$q' \mathbf{P}^{-1} \mathbf{H}^T = (q \mathbf{S}\mathbf{G} + \epsilon') \mathbf{H}^T = \epsilon' \mathbf{H}^T \quad (8)$$

by construction. Because $\|\epsilon'\| \leq (d-1)/2$, one can identify ϵ' and remove it from the permuted message and therefore recover $q\mathbf{S}$. Finally, the encoded message can be recovered by multiplying \mathbf{S}^{-1} to the right of $q\mathbf{S}$.

Without the knowledge of the private key, the message q' can be decoded by using the maximum likelihood estimation:

$$q = \operatorname{argmin}_{x \in \mathbb{F}_2^k} \|q' - x \mathbf{G}'\|. \quad (9)$$

Recalling that Eq. (9) is invariant by non-singular transformations $x \leftarrow x \mathbf{Q}$ with $\mathbf{Q} \in \mathbb{F}_2^{k \times k}$, it is always possible to reduce \mathbf{G}' to its normal form $\mathbf{Q}^{-1} \mathbf{G}' = (\mathbb{1} \mathbf{W})$, with $\mathbb{1}$ being the identity matrix of size $k \times k$ and $\mathbf{W} \in \mathbb{F}_2^{k \times (N-k)}$.

Since the encrypted message q is recoverable, it is guaranteed that one and only one configuration exists that minimizes Eq. (9). The hardness of the McEliece protocol depends on the size of the codespace and the distance d of the code C . By properly choosing k and d , it is possible to generate instances with a tunable hardness.

IV. GENERATING HARD INSTANCES FROM LINEAR CODES

In this section we will show that the McEliece protocol can be used to generate hard instances of a disordered Ising Hamiltonian. More precisely, we are interested in generating p -local Ising instances of the form:

$$H(\sigma) = \sum_{i=1}^M J_i \sigma_{i_1} \cdots \sigma_{i_p} \quad (10)$$

with $p \geq 1$, $1 \leq i_1, \dots, i_p \leq k$, $\sigma = \{\pm 1\}^k$ and couplings $J_{i_1 \dots i_p} \in \mathbb{R}$. To achieve this goal, it suffices to show that finding a solution of the maximum likelihood equation in Eq. (9) is equivalent to finding the ground state of the p -local Ising instance (10). This equivalence is well-known in the theory of spin glasses and has motivated statistical-mechanical studies of various error correcting codes [49, 50].

Let us define \mathbf{G}'_i the i -th column of \mathbf{G}' . Therefore, it is immediate to show that:

$$W(x) = \|q' - x \mathbf{G}'\| = \sum_{i=1}^N \|q'_i - x \cdot g'_i\|, \quad (11)$$

where the operations inside $\|\cdot\|$ are intended modulo 2, while the sum is over \mathbb{R} . By mapping $\sigma_i = 1 - 2x_i$, and by recalling that

$$(x_1 + \cdots + x_k) \bmod 2 = (1 - \sigma_1 \cdots \sigma_k)/2, \quad (12a)$$

$$(x_1 + \cdots + x_k + 1) \bmod 2 = (1 + \sigma_1 \cdots \sigma_k)/2, \quad (12b)$$

Eq. (11) becomes:

$$\begin{aligned} W(x) &= \sum_{i=1}^N \|q'_i - x \cdot \mathbf{G}'_i\| = \sum_{i=1}^N \left[1 - (-1)^{q'_i} \sigma_{i_1} \cdots \sigma_{i_{p_i}} \right] \\ &= - \sum_{i=1}^N (-1)^{q'_i} \sigma_{i_1} \cdots \sigma_{i_{p_i}} + N = H(\sigma) + N, \end{aligned} \quad (13)$$

with $\{i_1, \dots, i_{p_i}\}$ being the indices of the non-zero elements of \mathbf{G}'_i , and $p_i = |g'_i|$ their number. It is interesting to observe that the indices of the interactions $\{i_1, \dots, i_{p_i}\}$ are fixed after choosing the private key $\{\mathbf{G}, \mathbf{H}, \mathbf{P}, \mathbf{S}\}$. However, multiple random instances can be generated by providing different $q' = q\mathbf{G}' + \epsilon$, which will only change the sign of the interactions. It is important to emphasize that, if the private key is properly chosen, every instance $H(\sigma)$ will be hard to optimize, regardless of the choice of q' . This is consistent with the fact that p -local instances with randomly chosen $J_{i_1 \dots i_p} = \pm 1$ and $p \geq 2$ are NP-Complete. However, unlike the case when the couplings are randomly chosen, p -local instances generated using the McEliece protocol have a *guaranteed* unique optimal value, which is known in advance (that is, q).

Since we don't need to apply \mathbf{S}^{-1} to obtain $H(\sigma)$ in Eq. (13), we can relax the request to have the obfuscation matrix \mathbf{S} be non-singular. In particular, the number of solutions of the $H(\sigma)$ will depend on the size of the kernel of \mathbf{S} . Indeed, not having \mathbf{S} invertible implies that \mathbf{S} has a non-empty kernel and, therefore, two distinct messages q_1 and q_2 may have the same encrypted message, q'_1 and q'_2 . Consequently, the p -local instance $H(\sigma)$ will have as many optimal configurations as the number of collisions for a given message q , that is the number of elements in the \mathbf{S} kernel.

A. Reduction to the 2-local Ising Model

Since the p -local Ising model is NP-Complete for $p \geq 2$, any optimization problem in the NP class can be mapped onto it. However, almost all post-Von Neumann [7–10] technologies can only optimize p -local Ising instances with either $p = 2$ or $p = 3$. Unfortunately, because of the random scrambling induced by \mathbf{S} , \mathbf{G}' is a dense matrix with $p_i \leq k$. Luckily, p -local couplings with $p > 3$ can always be reduced to $p \leq 3$ by adding auxiliary variables.

For $p > 3$, it is immediate to show that:

$$\begin{aligned} &(-1)^t \sigma_1 \cdots \sigma_l \sigma_{l+1} \cdots \sigma_p = \\ &\min_{\omega = \pm 1} \left[\sigma_1 \cdots \sigma_l \omega + (-1)^t \omega \sigma_{l+1} \cdots \sigma_p \right] + 1. \end{aligned} \quad (14)$$

Therefore, reducing \mathbf{G}' to a 3-local Ising instance would require no more than $k' = k + (\lceil \frac{k}{2} \rceil - 1)(N - k)$ spin variables and $n' = k + \lceil \frac{k}{2} \rceil (n - k)$ couplings in the worst case scenario. Reducing a coupling from $p = 3$ to $p = 2$

requires the addition of another extra auxiliary spin for each 3-local coupling. More precisely, since

$$\begin{aligned} \operatorname{argmin}_{\sigma_1, \sigma_2, \sigma_3 = \pm 1} (-1)^t \sigma_1 \sigma_2 \sigma_3 = \\ \operatorname{argmin}_{\sigma_1, \sigma_2, \sigma_3, \omega = \pm 1} [\sigma_1 + \sigma_2 + (-1)^t (1 - 2\omega)]^2, \end{aligned} \quad (15)$$

it is possible to reduce \mathbf{G}' to up to $k'' \equiv k(N - k + 1) = \mathcal{O}(kN)$ spin variables and $N'' \equiv N + k(n - k) = \mathcal{O}(kN)$ couplings in the worst case scenario.

B. The Scrambling Protocol

In this Section we will show how we can use the “scrambling” of the codespace of C induced by the non-singular matrix \mathbf{S} to generate random hard p -local Ising instances with a known optimal configuration. To this end, it suffices to show that any p -local Ising instance of the form Eq. (10) can always be reduced to a maximum likelihood problem as in Eq. (9).

Using the transformation in Eq. (12), the p -local Ising instance in Eq. (10) can be rewritten as:

$$H(x) = \sum_{i=1}^M \operatorname{abs}(J_i) \left(\left\| x_i + \dots + x_{i_p} + \frac{1 + \operatorname{sgn}(J_i)}{2} \right\| - 1 \right), \quad (16)$$

where $\operatorname{abs}(\cdot)$ and $\operatorname{sgn}(\cdot)$ are the absolute and sign functions respectively, and all operations inside $\|\cdot\|$ are modulo 2. If we define $\mathbf{J} \in \mathbb{F}_2^{k \times M}$ the adjacency matrix of the couplings $J_{i_1 \dots i_p}$ such that $\mathbf{J}_{ai} = 1$ if $a \in \{i_1, \dots, i_p\}$ and zero otherwise, Eq. (16) becomes

$$H(x) = \sum_{i=1}^M \operatorname{abs}(J_i) \left(\left\| x \cdot \mathbf{J}_i + \frac{1 + \operatorname{sgn}(J_i)}{2} \right\| - 1 \right), \quad (17)$$

where \mathbf{J}_i is the i -th column of \mathbf{J} and $x \in \mathbb{F}_2^k$. Observe that Eq. (17) is equivalent to the maximum likelihood in Eq. (9) when $\operatorname{abs}(J_i) = 1$ for all i . More importantly, it is immediate to see that, for any non-singular transformation, \mathbf{S} an optimal configuration x^* of $H(x)$ is mapped to $x'^* = x^* \mathbf{S}^{-1}$, preserving the number of optimal configurations. We can relax the condition of having \mathbf{S} being non-singular. In this case, the number of optimal configurations is not preserved since

$$x^* = (x'^* + \xi) \mathbf{S} \quad (18)$$

for any ξ belonging to the kernel space of \mathbf{S} . Once the adjacency matrix $\mathbf{J}' = \mathbf{S} \mathbf{J}$ is scrambled, one can map Eq. (17) back to a p -local Ising instance using the methodology presented in Section IV A.

In the next Section we try to shed light on the reason why scrambling the configuration space x with \mathbf{S} produces instances which are hard to optimize for local heuristics.

V. RANDOM SCRAMBLING OF ENERGY LANDSCAPES

In order to study the effect of energy scrambling over an Ising Hamiltonian, we show in this Section how various forms of energy scrambling — similar to the one induced by the scrambling matrix \mathbf{S} of the McEliece protocol — can transform simple problems into significantly more complex ones by introducing a version of a phenomenon known in the statistical physics literature as “clustering” [51, 52], where the solution space of a constraint optimization problem splits into a (typically exponential) number of “clusters”. This phenomenon is conjectured — on the basis of empirical evidence collected in the study of constraint satisfaction problems — to impair the performance of stochastic local search algorithms such as WalkSAT [53] even though the precise connection between clustering and the theory of algorithmic hardness is still an active area of research, and not fully understood [54, 55].

In order to understand the algorithmic hardness of the system of Eq. (10) using the methods of statistical physics, one would like to study the typical properties of the energy landscape of the “disordered Hamiltonian” $H(\sigma)$ where the disordered couplings $J_{i_1 \dots i_p}$ are generated by *e.g.* a fixed choice of the linear code matrix \mathbf{G} (one for each system size N), and the random choices for the permutation matrices \mathbf{S}, \mathbf{P} . For this introductory work we limit ourselves to a simpler scenario that allows us focusing on one component of the McEliece protocol: the effect of an energy scrambling matrix \mathbf{S} . In particular

1. We only consider the effect of one source of quenched disorder, *i.e.* a random scrambling matrix \mathbf{S} . As shown in Section IV B, the effect of changing the \mathbf{S} permutation matrix in the McEliece protocol (for given \mathbf{G} and \mathbf{P}) is to shuffle the energies of the states of the system.
2. Instead of considering the effects that \mathbf{S} has on the energy landscape of a reference Hamiltonian $H(\sigma)$ generated by fixed \mathbf{G} and \mathbf{P} , we use as a reference energy landscape a simple “convex” one that can be easily navigated by steepest descent.

We note that these simplifications, while creating some disconnect with the McEliece Hamiltonian, have the advantage of making the scrambling protocol of broader application to more generic Ising spin models. We leave a complete analysis of the McEliece Hamiltonian for future work.

The main results of this section show that energy scrambling can generate clustered (empirically “hard”) landscapes from unclustered (empirically “easy”) ones. In order to review the concept of clustering, let us assume that we have some disordered Hamiltonian H_J (dependent on some quenched disorder J) over a system of N Ising spins, so that each $\sigma \in \{\pm 1\}^N$ is assigned an energy E_σ . For a given energy density $\epsilon = E/N$ and value of

the fractional Hamming distance $x = X/N \in [0, 1]$, one defines the quantity:

$$\mathcal{N}(x, \epsilon) \equiv \sum_{\sigma, \tau} \delta(d_{\sigma, \tau} - xN) \delta(E_{\sigma} - \epsilon N) \delta(E_{\tau} - \epsilon N), \quad (19)$$

where the double sum is over all spin configurations $\sigma, \tau \in \{\pm 1\}^N$, $d_{\sigma, \tau}$ is the Hamming distance between σ and τ , E_{σ}, E_{τ} are the energies of the configurations, and $\delta(y)$ are Kronecker delta functions (meaning that $\delta(y) = 1$ if $y = 0$, and $\delta(y) = 0$ otherwise).

For a given realization of disorder, this function computes the number of pairs of spin configurations $\sigma, \tau \in \{\pm 1\}^N$ such that

1. σ, τ are exactly xN spin flips away from each other
2. both σ and τ have the same energy ϵN

This means that $\mathcal{N}(\epsilon) \equiv \int_0^1 \mathcal{N}(x, \epsilon) dx$ is a quadratic function of the number of states of given energy density ϵ . In many spin glass models and constraint satisfaction problems one expects that the number of states of given energy density should be of exponential order in N , and consequently one should have $\mathcal{N}(x, \epsilon) \sim \exp(N\Phi_{x, \epsilon} + o(N))$ for some N -independent real number $\Phi_{x, \epsilon}$.

The main observation here is that there can exist energy densities ϵ such that for some values of x , $\mathcal{N}(x, \epsilon) \rightarrow 0$ as $N \rightarrow \infty$, while for other values x' , $\mathcal{N}(x', \epsilon)$ diverges with N . This means that in the thermodynamic limit, the spin configurations that populate the micro-canonical shell of energy ϵN are not arbitrarily close or far away from each other, but can exist only at some given distances. Indeed, with increasing x from zero to one, the quantity $\mathcal{N}(x, \epsilon)$ typically has a diverging region (for x between 0 and some x_1), followed by a region where $\mathcal{N}(x, \epsilon) \rightarrow 0$ (that we call a “forbidden region”), followed by a revival of the divergent behavior (from $x_2 > x_1$ to 1).

The emerging picture is that these configurations form extensively-separated “clusters”, where configurations included in the same cluster can be connected by “jumping” along a sequence of configurations (all belonging to the energy shell), each $\mathcal{O}(1)$ spin flips away from the previous one, while configurations belonging to different clusters require an extensive number of spin flips.

In a disordered system the quantity $\mathcal{N}(x, \epsilon)$ will depend on the disorder realization, so one is led to studying some statistics of $\mathcal{N}(x, \epsilon)$, the easiest being its disorder-averaged value

$$\begin{aligned} \langle \mathcal{N}(x, \epsilon) \rangle &= \sum_{\sigma, \tau} \delta(d_{\sigma, \tau} - xN) \langle \delta(E_{\sigma} - \epsilon N) \delta(E_{\tau} - \epsilon N) \rangle \\ &= 2^N \binom{N}{xN} \Pr [E_{\sigma} = \epsilon N, E_{\tau} = \epsilon N], \end{aligned} \quad (20)$$

where we have used the fact that the expectation value of the indicator function of an event is equal to the probability of that event. Then the meaning of $\langle \mathcal{N}(x, \epsilon) \rangle \rightarrow 0$ for

$N \rightarrow \infty$ is that the probability of finding disorder realizations with at least one pair of states satisfying conditions 1. and 2. above, is vanishing as one approaches the thermodynamic limit. This is because while the expectation value of a variable is not necessarily a good indicator of its typical behavior, since $\mathcal{N}(x, \epsilon)$ is a non-negative random variable one can use Markov’s inequality to show that for any $\alpha > 0$

$$\Pr [\mathcal{N}(x, \epsilon) > \alpha] \leq \frac{1}{\alpha} \langle \mathcal{N}(x, \epsilon) \rangle, \quad (21)$$

so that when $\langle \mathcal{N}(x, \epsilon) \rangle \rightarrow 0$ in the large- N limit (*i.e.* in the forbidden regions) then the distribution of $\mathcal{N}(x, \epsilon)$ is also increasingly concentrated in zero, and behaves like a Dirac delta in the thermodynamic limit. So the average and typical behavior coincide (in the thermodynamic limit) at least inside of the forbidden regions, which is enough for us to establish the existence of clustering.

Observe that, in all models we consider, the expectation value $\langle \mathcal{N}(x, \epsilon) \rangle$ decays exponentially to zero inside of the forbidden regions, as a function of the system size N in the asymptotic regime $N \rightarrow \infty$. Therefore, the likelihood of generating an instance with pairs of states at given distance x and energy ϵ , for (x, ϵ) values inside the forbidden region (that is, an “unclustered” instance), is also exponentially small.

A. The Hamming-Weight Model

As an example, consider the Hamming-Weight Model (HWM) defined by the Hamiltonian [56]:

$$H(\sigma) = -\frac{1}{2} \sum_{i=1}^N (\sigma_i - 1). \quad (22)$$

This is a non-disordered Hamiltonian and $\mathcal{N}(x, \epsilon)$ can be computed directly. Note that the triangle inequality for the Hamming distance implies that unless we have that $x/2 \leq \min(\epsilon, 1 - \epsilon)$, then $\mathcal{N}(x, \epsilon) = 0$. Assuming this inequality to hold, then

$$\begin{aligned} \mathcal{N}(x, \epsilon) &= \binom{N}{\epsilon N} \binom{\epsilon N}{\frac{1}{2}xN} \binom{(1 - \epsilon)N}{\frac{1}{2}xN} \\ &= \exp \left\{ N \left[S(\epsilon) + \epsilon S\left(\frac{x}{2\epsilon}\right) + (1 - \epsilon) S\left(\frac{x}{2(1 - \epsilon)}\right) \right] + o(N) \right\}, \end{aligned} \quad (23)$$

where we have used Stirling’s approximation to show that for $0 \leq p \leq 1$ one has $\binom{N}{pN} = \exp(NS(p) + o(N))$ where $S(p) \equiv -p \ln(p) - (1 - p) \ln(1 - p)$ is the binary Shannon entropy.

Note that in this case the $\mathcal{O}(N)$ prefactor $\Phi_{x, \epsilon}$ at the exponent is

$$\begin{aligned} \Phi_{x, \epsilon} &= \lim_{N \rightarrow \infty} \frac{1}{N} \ln \mathcal{N}(x, \epsilon) \\ &= S(\epsilon) + \epsilon S\left(\frac{x}{2\epsilon}\right) + (1 - \epsilon) S\left(\frac{x}{2(1 - \epsilon)}\right), \end{aligned} \quad (24)$$

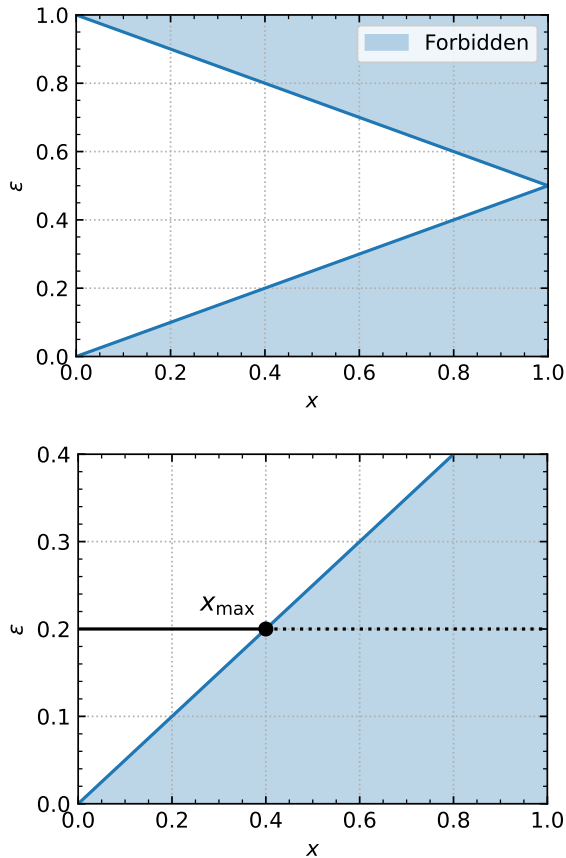


FIG. 1. (Top) (x, ϵ) -phase diagram of the HWM. The energy density of the HWM is contained in $0 \leq \epsilon \leq 1$, and the fractional Hamming distance is $0 \leq x \leq 1$. The regions shaded in blue are given by the points (x, ϵ) where $\mathcal{N}(x, \epsilon)$ is exactly zero at any given size. (Bottom) Zoomed-in detail of the (x, ϵ) -phase diagram around the energy density $\epsilon = 0.2$. Pairs of configurations with this energy density exist at any distance below $x_{\max} = 2\epsilon$, and none above. This implies that the configurations with this energy density form one single cluster of radius x_{\max} .

which is never negative since $0 \leq S(p) \leq \ln 2$. Notice that even though the existence of values x, ϵ where $\mathcal{N}(x, \epsilon) = 0$ does mean that there are forbidden regions in the (x, ϵ) -phase diagram of this model, the presence of these regions does not entail clustering. This is because for any given value of ϵ , the forbidden region starts at some $x_{\max} > 0$ and then extends all the way to $x = 1$. This implies that the configurations with energy ϵN cannot exist at a separation larger than x_{\max} but appear at all distances below that, *i.e.* they form one single cluster of radius x_{\max} . Therefore the HWM does not exhibit clustering (see Fig. 1).

B. The Randomly-Permuted Hamming-Weight Model

The Randomly-Permuted Hamming-Weight Model (RPHWM) is a disordered system obtained by taking the HWM and giving a random permutation to the configurations, while keeping their original energies fixed. Formally, for a fixed number of spins N , one samples a random element $\pi \in S_{2^N}$ of the permutation group over 2^N objects, uniformly at random. Then defines the energy E_σ of a given spin configuration $\sigma \in \{\pm 1\}^N$ as $E_\sigma \equiv \|\pi(\sigma)\|$ where $\|\cdot\|$ is the Hamming weight norm. This model was introduced in [57].

Sampling the disorder ensemble of the RPHWM can be recast as a process of extraction from an urn without replacement, where the 2^N spin configurations are given some canonical (*e.g.* lexicographic) ordering $S^{(1)}, \dots, S^{(2^N)}$, and the urn contains all the possible values of the energies of the HWM with their multiplicities. These energies are randomly assigned to the configurations by extracting them sequentially from the urn, the first energy going to the configuration $S^{(1)}$, the second to $S^{(2)}$ and so on. Following this equivalent reformulation, then one can easily compute

$$\begin{aligned} \langle \mathcal{N}(x, \epsilon) \rangle &= 2^N \binom{N}{xN} \frac{1}{2^N} \binom{N}{\epsilon N} \frac{1}{2^N - 1} \left[\binom{N}{\epsilon N} - 1 \right] \\ &= \frac{1}{2^N - 1} \binom{N}{xN} \binom{N}{\epsilon N}^2 - \frac{1}{2^N - 1} \binom{N}{xN} \binom{N}{\epsilon N} \\ &\sim \exp \left[N \left(-\ln(2) + S(x) + 2S(\epsilon) \right) + o(N) \right]. \end{aligned} \quad (25)$$

Now we have that

$$\Phi_{x,\epsilon} = -\ln(2) + S(x) + 2S(\epsilon) \quad (26)$$

is negative iff

$$S(\epsilon) < \frac{\ln(2) - S(x)}{2}. \quad (27)$$

This inequality can be solved numerically to obtain a plot of the forbidden regions in the (x, ϵ) -phase diagram of the RPHWM (see Fig. 2). Setting $S(x) = 0$ we obtain that forbidden regions start appearing at energy densities ϵ that satisfy $S(\epsilon) < \ln(2)/2$ which for low-energy states happens around $\epsilon \approx 0.11$.

Notice that to properly establish clustering, one would normally need to perform second-moment calculations in order to rule out the possibility that the forbidden regions at a given energy density ϵ span the *entire* interval $0 \leq x \leq 1$ (first-moment calculations can be used to prove the absence of states for given (x, ϵ) but not their presence). Such a case would not indicate clustering, but simply the absence of states at that given ϵ for the model under study. In our case second-moment calculations are unnecessary since we know that scrambling – being a permutation of the states – leaves unchanged the number of pairs of states one can have at a given energy

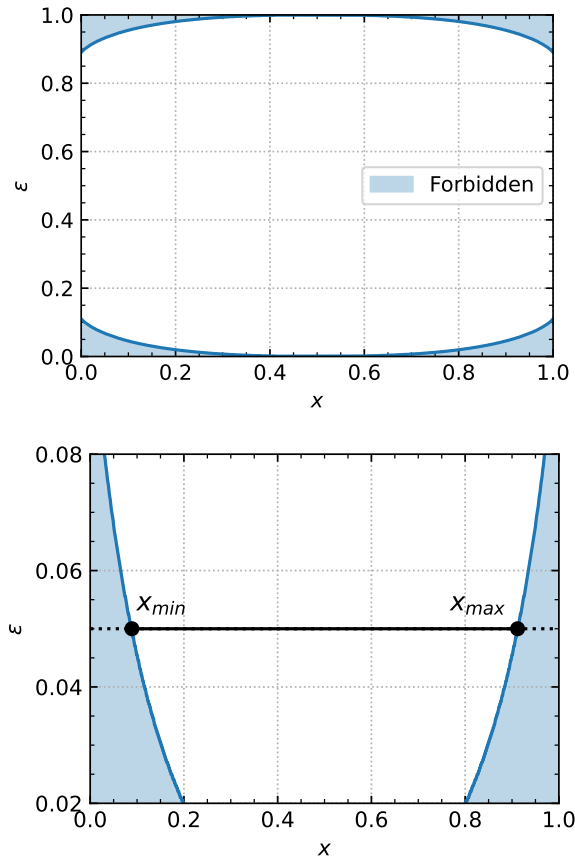


FIG. 2. (Top) (x, ϵ) -phase diagram of the RPHWM. The regions shaded in blue are given by the points (x, ϵ) where $\mathcal{N}(x, \epsilon)$ goes to zero in the thermodynamic limit. (Bottom) Zoomed-in detail of the (x, ϵ) -phase diagram around the energy density $\epsilon = 0.05$. Pairs of configurations with this energy density cannot exist at a distance smaller than x_{\min} or larger than x_{\max} . Thus, x_{\min} can be interpreted as the smallest separation between the clusters, and each cluster has zero diameter (both in fractional Hamming distance).

density $\mathcal{N}(\epsilon) = \int_0^1 \mathcal{N}(x, \epsilon) dx$, which we can compute in the HWM and is always positive for $\epsilon \in [0, 1]$. Thus, the absence of states at energy density ϵ is impossible, and the existence of forbidden regions implies clustering.

Notice, moreover, that the clusters will typically include only a sub-exponential number of states (their diameter being zero in fractional Hamming distance [58]) and therefore most of the spin variables will be *frozen*: starting from a state in a cluster, flipping any such variable will necessarily move you out of the cluster. The presence of an extensive number of frozen variables in the set of solutions has been proposed as the reason behind the hardness of constraint satisfaction problems over random structures [52, 59, 60]. Here we do not attempt to develop a formal connection between frozen variables and the algorithmic hardness of our model, but leave such considerations for future works.

C. The Linearly-Scrambled Hamming-Weight Model

Let us define how one generates the energies of the states in a disorder realization of the Linearly-Scrambled Hamming-Weight Model (LSHWM). This is more easily described by passing to the binary representation of the spin configurations, *i.e.* by defining the variables $x_i \equiv (1 - \sigma_i)/2$ so that each spin configuration $(\sigma_1, \dots, \sigma_N) \in \{\pm 1\}^N$ is mapped to a binary string $(x_1, \dots, x_N) \in \mathbb{F}_2^N$ (see Eq. (12)). In order to generate a disorder realization of the LSHWM for a system of N spins, one samples N^2 numbers $a_{ij} \in \{0, 1\}$ with $1 \leq i, j \leq N$ according to the symmetric probability distribution $\Pr[a = 0] = \Pr[a = 1] = 1/2$, and defines the “scrambling matrix” $\mathbf{S} \in \mathbb{F}_2^{N \times N}$ by using the $\{a_{ij}\}$ as its entries: $\mathbf{S}_{ij} = a_{ij}$. Then every string $X = (x_1, \dots, x_N)$, taken as a column vector in \mathbb{F}_2^N , is mapped to some new string $X' \in \mathbb{F}_2^N$ according to the rule

$$\begin{bmatrix} x'_1 \\ \vdots \\ x'_N \end{bmatrix} = \mathbf{S} \begin{bmatrix} x_1 \\ \vdots \\ x_N \end{bmatrix}, \quad (28)$$

(where matrix-vector multiplication is defined in \mathbb{F}_2) and then we define the energy E_σ (that is, the energy of the spin configuration σ represented by the binary string X) to be the Hamming weight of the vector X' .

In the Appendix we compute, for $x, \epsilon > 0$, the probability

$$\Pr \left[E_\sigma = \epsilon N, E_\tau = \epsilon N \right] \equiv P_\epsilon = 2^{-2N} \binom{N}{\epsilon N}^2 \quad (29)$$

for two configurations $\sigma, \tau \in \{\pm 1\}^N$, neither of which is the “all-spins-up” configuration (represented by the zero vector in \mathbb{F}_2^N , for which a positive energy density is forbidden by linearity). Then it becomes easy to show that

$$\begin{aligned} \langle \mathcal{N}(x, \epsilon) \rangle &= \sum_{\sigma, \tau} \delta(d_{\sigma, \tau} - xN) \Pr \left[E_\sigma = \epsilon N, E_\tau = \epsilon N \right] \\ &= \sum_{\sigma \neq 0} \sum_{\tau \neq 0} \delta(d_{\sigma, \tau} - xN) P_\epsilon \\ &= (2^N - 1) \left[\binom{N}{xN} - 1 \right] P_\epsilon \\ &\sim 2^N \binom{N}{xN} P_\epsilon \\ &= \exp \left[N \left(-\ln(2) + 2S(\epsilon) + S(x) \right) + o(N) \right] \quad (30) \end{aligned}$$

therefore

$$\Phi_{x, \epsilon} = 2S(\epsilon) + S(x) - \ln(2), \quad (31)$$

which is negative if and only if

$$S(\epsilon) < \frac{\ln(2) - S(x)}{2}, \quad (32)$$

exactly as in the RPHWM. Therefore their clustering phase diagrams are the same.

Note that unlike the previous case, the particular ensemble of scrambling matrices used here includes non-invertible matrices and, as a consequence, the uniqueness of the ground state of the model is not guaranteed. However, provided the typical rank of the scrambling matrix scales like $\mathcal{O}(N)$, then the fraction of ground states $2^{N-\text{rank}(\mathbf{S})}/2^N$ in the system is exponentially decaying with N , so these cannot be easily found just by *e.g.* a polynomial number of random guesses. We refer to Appendix A where we summarize the results the literature, which show that in the limit of large- N the typical nullity of our scrambling matrices converges to a finite value. Thus, by the rank-nullity theorem, their typical rank must be $\mathcal{O}(N)$.

VI. SIMULATIONS OF HARD SCRAMBLED INSTANCES

With an understanding of why local search heuristics are ineffective for a scrambled Hamiltonian, we will now aim to measure the hardness of scrambled instances generated with a cryptographically realistic family of public/private key pairs for the McEliece protocol. While the RPHWM may appear statistically hard, a more clever optimizer can use the knowledge that the underlying Hamiltonian is the HWM to directly calculate \mathbf{S} from the terms of the scrambled Hamiltonian with some simple linear algebra and completely side-step the need to directly optimize it. Thus, it is necessary to consider a family of *cryptographically hard* linear error correcting codes which (loosely defined for our purposes) possess a generator matrix \mathbf{G} that cannot be easily recovered from its scrambled generator matrix \mathbf{G}' when used in the McEliece protocol, even with knowledge of how \mathbf{G} could be generated. In other words, algorithmic backdoors to optimizing a scrambled Hamiltonian are prevented by the very cryptanalysis that quantifies how difficult it is to break the McEliece protocol (*i.e.* solving for the message q in Eq. (9)) using the best known attacks.

We will first briefly review the overall approach most often applied for breaking the McEliece protocol, focusing on Stern's algorithm and its success probability. We will then present numerical benchmarks comparing the scaling of a local search algorithm against Stern's algorithm. We empirically show that local search on cryptographically hard McEliece instances exhibit an exponential scaling $\mathcal{O}(2^k)$ for the time-to-solution, no better than exhaustive enumeration and consistent with the presence of clustering. Since N and k are related by the code rate $R = k/N$, local search has an equivalent scaling of $\mathcal{O}(2^{RN})$, which is asymptotically $\mathcal{O}(2^N)$ in the worst case that $R \rightarrow 1$ as $N \rightarrow \infty$ (as is the case in this section). On the other hand, the exponential scaling of Stern's algorithm is $\mathcal{O}(2^{cN})$, where $c = 0.05564$ is the theoretical worst-case exponential constant (for any underlying

code rate R) and we obtain a numerical scaling consistent with this exponent. We establish here a concrete benchmarking parameter regime using cryptographically hard Ising instances with a demonstrably ample gap to close between algorithms and Ising devices relying on local search and the cryptanalytic state-of-the-art.

A. Information Set Decoding and the Stern Algorithm

An *information set* of an $[N, k, t]$ code is a subset $I \subset \{1, \dots, N\}$ of size k such that $G|_I$, the square sub-matrix formed by the columns of G indexed by I , is invertible. That is, if no errors exist on the bits in the information set, then the message is successfully decoded using only $G|_I$. A *redundancy set* is a subset $R \subset \{1, \dots, N\}$ of size $N - k$ such that $H|_R$, the square sub-matrix of columns of H indexed by R , is invertible. Said similarly, if all of the errors occur on a redundancy set, then they can be uniquely identified. Clearly, for any two disjoint sets I and R such that $I \cup R = \{1, \dots, N\}$, I is an information set if and only if R is a redundancy set.

The algorithmic approach of finding an error-free (or nearly error-free) information set to decode a message is called *information set decoding* (ISD). Such algorithms constitute a general attack on cryptosystems based on linear codes, as they make no assumptions concerning the structure of the underlying code. After the generator matrix \mathbf{G}' is mapped to a p -local Hamiltonian via Eq. (13), an ISD algorithm can be seen as an Ising optimization algorithm that is based on searching for a partition of the summed Ising terms such that all unsatisfied couplings (or as many unsatisfied couplings as possible) in Eq. (13) belong to the redundancy set. The most naïve but illustrative ISD algorithm is to simply select k out of N bits at random from the encoded message and check if they are an error-free information set by attempting Gaussian elimination. Suppose that we are trying to decode a message with t errors (typically $t = \lfloor (d - 1)/2 \rfloor$, the maximum error-correcting capacity of the code). The probability that this random selection is successful is

$$P_{\text{succ,ISD}} = \frac{\binom{N-t}{k}}{\binom{N}{k}}. \quad (33)$$

Since the distance of a code can grow with its size, the maximum correctable distance t does not remain fixed (potentially $t = \mathcal{O}(N)$), so the worst-case cost increases as $\mathcal{O}(2^{cN})$ where c is a constant that generally depends on the code rate $R = k/N$ as $N \rightarrow \infty$ for the particular family of codes being decoded. However, c is maximized over all code rates $0 < R < 1$ to yield the worst-case exponential scaling with N for a specific algorithm using any underlying code for the McEliece protocol, regardless of its rate R or its error correcting distance t [61].

Stern's algorithm [62, 63] is a refinement of ISD that relaxes the requirement that all of the error bits are

found in the redundancy set; instead, only $t - 2p$ of the errors are required, where $p \geq 1$ is an integer parameter of the algorithm (not to be confused with the indefinite p of a p -local Hamiltonian). The remaining $2p$ errors are searched for by splitting the information set into two random partitions (I_1 and I_2) and then computing linear combinations of columns consisting of exactly p columns from I_1 and p columns from I_2 . An iteration of Stern’s algorithm is thus successful if exactly $2p$ error bits are assigned to the information set, and then exactly p error bits are assigned into each of the two partitions. Thus, the success probability of one iteration of Stern’s algorithm can be calculated to be

$$P_{\text{succ,Stern}} = \frac{\binom{t}{2p} \binom{N-t}{k-2p} \left(\frac{k/2}{p}\right)^2}{\binom{N}{k} \binom{k}{2p}}. \quad (34)$$

Stern’s algorithm is generally practical with either $p = 1$ or 2. A detailed description of Stern’s algorithm and other ISD algorithms is given in Appendix C. While there have been more sophisticated combinatorial refinements of ISD in recent literature, Stern’s algorithm is almost as simple to implement as plain ISD, and all further improvements proposed to date have only resulted in marginally improved worst-case scaling from $O(2^{0.05564N})$ for Stern’s algorithm to just $O(2^{0.04934N})$ at the cost of additional—but substantial—complexity to implement [61].

It should be emphasized that this scaling behavior relies on a choice of code family that does not have enough structure to infer from the public key, but at the same time should have an efficient decoding algorithm up to t errors using the private key. The most successful such family is the Goppa codes, whose codewords are based on randomly selected elements of a finite field. This is the very same family originally proposed by McEliece [45] and has resisted the discovery of a breaking attack to this day [46].

B. Benchmarking Parallel Tempering Monte Carlo on McEliece Instances

Having established the asymptotic scaling of the best known cryptographic attacks on secure implementations of the McEliece protocol, we will now examine how parallel tempering (PT) Monte Carlo [64–66], one of the most effective heuristics with local-search moves for Ising spin glasses, performs at finding the ground state of the corresponding scrambled Hamiltonian (*i.e.* McEliece instances). As summarized above, we will show that the scaling of PT is substantially separated from the theoretical scaling of an ISD attack on the cryptosystem and interpret this separation as evidence of clustering.

Computational Implementations. We randomly generated McEliece instances, defined by the scrambled \mathbf{G}' matrix and encoded q' vector, as described in Appendix D. Every instance consists of both a random

Goppa code and a random binary message of length k . We developed our implementations of Stern’s algorithm, which uses the parity check matrix \mathbf{H} and syndrome z of the McEliece instance as its input, as well as PT Monte Carlo for sampling a binomial ($J = \pm 1$) p -local Ising Hamiltonian, using \mathbf{G}' and q' as input directly. Each replica of PT Monte Carlo directly samples the p -local Hamiltonian with Metropolis Monte Carlo moves, and not the reduction of the p -local Hamiltonian to a 2-local Hamiltonian. We do this to ensure we are close to the “best case” scenario of resource requirements for a local algorithm. Details of the algorithm are given in Appendix C. Our implementations are written in C++ and target x86 CPU architectures. Since iterations of Stern’s algorithm are easy to parallelize, we also included support for MPI parallel workers. We performed all tests on identical Sandy Bridge Xeon E5-2670 processors and compiled our code using the Intel 2020 compiler with `-O3 -xAVX` optimization flags.

The original algorithm described by Stern includes an additional step that peeks at the sum of the selected columns on a small number of random rows and checks that it is zero before summing all $N - k$ rows. Theoretically, this significantly reduces the number of operations per iteration for a relatively small reduction in the success probability. However, we have omitted this step from our implementation as it adds a substantial amount of indirection within a hot loop and reduces the opportunity for vectorization when compiling to optimized CPU instructions, which are especially critical when vectors and matrices over \mathbb{F}_2 are bit-packed in memory. The performance of the original Stern algorithm was clearly not optimal for the sub-cryptographically secure parameter ranges we are interested in.

Our benchmark metric is the time-to-solution (TTS) at the 99% confidence level, *i.e.*

$$\text{TTS} = \tau \frac{\log(1 - 0.99)}{\log(1 - P_{\text{succ}})}, \quad (35)$$

where τ is the “cost” of each iteration, which can be measured in either the number of “elementary bit operations” or the CPU time per iteration. Our theoretical TTS of Stern’s algorithm simply takes τ to be the sum of the worst-case complexities of its two major stages: $(N - k)^3$ operations for inversion by Gaussian elimination plus $(N - k) \left(\frac{k}{2} Cp\right)^2$ operations for the combinatorial search for $2p$ error bits, yielding \log_2 TTS in bits of security. The formal analysis of the computational cost of cryptographic attacks is an ongoing area of development [67]. To measure the TTS of our implementation of Stern’s algorithm, we take τ to be the average measured CPU time per iteration and evaluate P_{succ} across all iterations on a single instance and estimate the error by the standard error of the mean TTS over all instances. The TTS of PT is evaluated by running PT until the ground state energy is found for 10 repetitions per instance, or up to 10^7 sweeps, ranking the total runtime required to find the solution of every run and finding the 99% quantile

across all repetitions and instances; the error estimate for the TTS is obtained by repeating this over bootstrap samples from the runtimes being ranked.

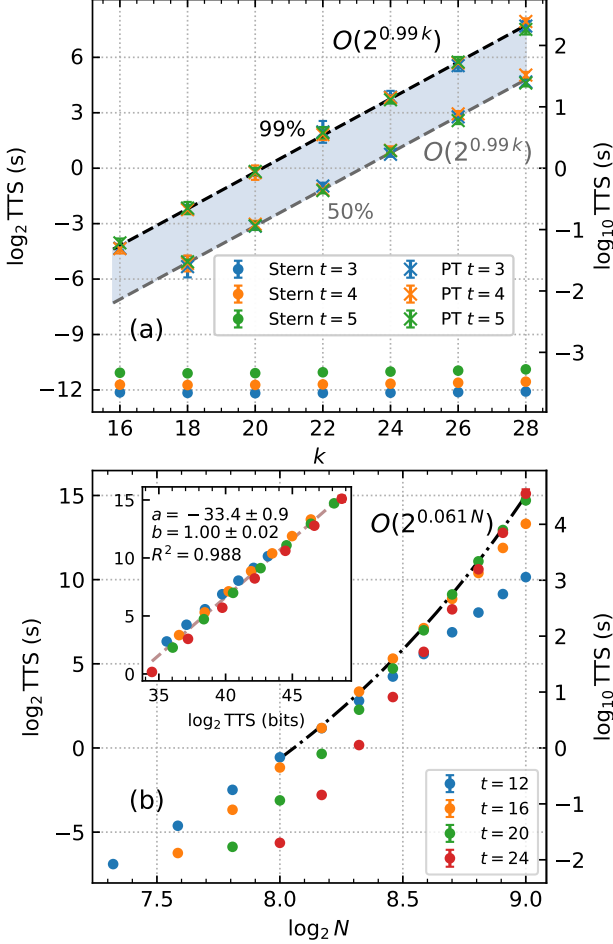


FIG. 3. Benchmark results of PT and Stern’s algorithm for solving Classic McEliece instances constructed from scrambled Goppa codes. (a) Comparison of PT and Stern’s algorithms at small error distances $t \in \{3, 4, 5\}$. The 99% and 50% quantiles of PT runtimes across all instance repetitions are both shown, with the area between the quantiles shaded. Both quantiles exhibit an exponential scaling of almost exactly $O(2^k)$, independently of code distance. The TTS (99%) of Stern’s algorithm rapidly outperforms PT (b) Performance of Stern’s algorithm at N sufficiently large to observe scaling behavior, with error distances $t \in \{12, 16, 20, 24\}$. The direct correlation between the measured and theoretical log-TTS of Stern’s algorithm with a linear fit (Measured log-TTS) = $a + b(\text{Theoretical log-TTS})$ is also verified (inset) The maximally hard code distances trace an exponential envelope of $O(2^{0.061N})$. Most error estimates for Stern’s algorithm are smaller than the plot marker size. All standard errors not specified are within ± 2 at the last significant digit. The finite fields of the Goppa codes were selected to avoid jumps in runtime (\mathbb{F}_2^8 in (a) and \mathbb{F}_2^9 in (b)).

The timing and TTS results are summarized in Fig. 3. For our first set of benchmarks, we examined a parameter regime where the TTS of PT was measurable with

tractable computational effort and its scaling could be extracted. We selected a finite field dimension of $m = 8$ and code sizes N such that $16 \leq k \leq 28$ across modest error-correcting distances $t \in \{3, 4, 5\}$ and generated 64 instances for each parameter combination.

In Fig. 3 (a), we observe a clear $O(2^k)$ scaling for PT that is virtually independent of the code distance, no better than the complexity of exhaustive enumeration. Even for as few as $k = 16$ spins, Stern’s algorithm is more competitive by a factor of about 100, though we performed 10^6 iterations of Stern’s algorithm for each instance to accurately measure the TTS. Furthermore, adjusting the code rate would only modulate the ratio of terms to variables in the Hamiltonian, which only has a polynomial effect through the time per iteration. Therefore, the TTS for PT is scaling as the worst-case scenario, that is proportionally to 2^k . While the complexity of PT is measured as function of k , this should be translated to a worst-case asymptotic as a function of the code size N for any possible that could be used with the McEliece protocol, regardless of its distance t or its code rate R . Since $R = k/N$ can be arbitrarily close to 1 in the worst case, this means the worst-case asymptotic of PT is $O(2^N)$, fully exponential in the code size. While selection of m was slightly larger than necessary to ensure that a broad parameter regime was accessible for scaling analysis, we ultimately limited the error correcting distance to $t \in \{3, 4, 5\}$ as neither algorithm behaves characteristically different in this range of k .

Fig. 3 (b) focuses on a more challenging parameter range for Stern’s algorithm using Goppa codes with $m = 9$, code sizes $160 \leq N \leq 512$, and a selection of $t \in \{12, 16, 20, 24\}$, which correspond to $40 \leq k \leq 404$ and are computationally inaccessible to PT. For this parameter range, we generated 32 instances for each parameter combination for the Goppa code. We performed between 1.6×10^6 and 51.2×10^6 iterations of Stern’s algorithm (distributed over 16 to 64 single-core MPI processes) for each instance as necessary to reduce the error estimates for increasing code sizes. We can see the worst-case exponential growth of the TTS by finding the hardest values of t for each code size. The measured exponential envelope of $O(2^{0.061N})$ scales slightly faster than the theoretical $O(2^{0.05564N})$ worst-case complexity of Stern’s algorithm, though not unexpectedly so since the TTS is almost, but not fully, in the asymptotic regime. Not only does Stern’s algorithm extend to a larger order of magnitude for k within a similar TTS as PT, but we have verified that its exponential scaling is far more tame.

We also observe a strong correlation between the predicted and measured TTS, verifying that our implementation correctly follows the success probability of Stern’s algorithm. This makes it possible to make a benchmark-driven prediction of the computational resources required for an implementation of Stern’s algorithm to succeed with a 99% probability, using a reasonable accounting method of bit operations. For example, a McEliece cryptosystem with a theoretical log-TTS of 64 bits will require

about 2×10^4 CPU-days to be broken with our implementation. This is not by any means a notable cryptographic benchmark. To emphasize the cryptographic hardness of the problem for much larger N , the smallest parameter set proposed for the Classic McEliece KEM is defined with $N = 3488$, $t = 64$, and a Goppa code finite field dimension of $m = 12$, which has a theoretical log-TTS of 159.7 bits. Even if parallelized over an exascale super-computer cluster such as Frontier, which has a theoretical peak performance of 1,679.82 petaflop/s, over 10^{22} years would still be required for Stern’s algorithm to succeed. Modest refinements of Stern’s algorithm reaching $O(2^{0.05N})$ scaling would not prevent an unrealistically large TTS. In any case, cryptographically hard McEliece instances establish a clear and rigorous CPU-timed upper bound for the worst-case performance of local search through Markov chain Monte Carlo on any class of scrambled problems.

Finally, recall our remark that the mapping of \mathbf{G}' to a scrambled Ising Hamiltonian yields an algorithmic picture where ISD is partitioning the Ising terms until the errors (unsatisfied terms in the ground state) can be singled out. Stern’s algorithm thus works in a picture where we search for $n - k$ terms of the Hamiltonian that contain most of the unsatisfied terms, perform a gauge transformation of the Hamiltonian (via Gaussian elimination) to extract a guess state, then attempt to check if it is $2p$ cluster moves (whose size scale with k) away from the ground state. The $O(2^k)$ scaling of PT that we have found is therefore consistent with a complete breakdown of local search due to clustering in the energy landscape of the Ising that separates the ground state from a typical excited state by an exponential number of moves. While Stern’s algorithm still scales exponentially, its complexity has a combinatorial origin and is not impeded by clustering.

Currently, the best quantum algorithm attack proposed to attack the McEliece cryptosystem is based on using Grover’s algorithm to speed up naive ISD by the usual Grover speedup [68]. However, without scalable universal fault-tolerant quantum computation, we do not expect any meaningful benchmarks of this approach to be possible in the near future using McEliece cryptographic instances. With present non-fault tolerant quantum devices, it is likely that only QAOA and quantum annealing would be the most suitable quantum optimization algorithms for such benchmarks. However, variational quantum algorithms such as QAOA are well-known to end up stuck optimizing in “barren plateaus” when implemented in noisy hardware [69]. Since Ising problems with clustering are already very unstructured, we expect they will also be problematic for this class of quantum algorithms. Finally, currently available quantum annealing hardware is limited to Ising Hamiltonians with 2-local couplings, which requires the use of additional qubits not only for the reduction from a p -local problem, but also for the minor-embedding of dense Hamiltonians. Nevertheless, investigating how to overcome these obstacles

and develop a careful scaling analysis of these quantum algorithms is a suitable subject for future work.

VII. CONCLUSION

In this work we have presented two main results. First, we have proposed a novel way of randomly generating instances of disordered Ising Hamiltonians with unique planted ground states by casting the public key of the McEliece cryptographic protocol as an interacting system of Ising spins. The algorithmic hardness of finding the ground state of the resulting Hamiltonians is equivalent to breaking the associated McEliece cryptosystem by only knowing its public key, while the private key allows the party who knows it to recover the planted ground state.

Secondly, in order to build some physical intuition as to the reason why our Hamiltonian model is hard to optimize beyond computational hardness assumptions of post-quantum cryptography, we have studied the effect of random energy-scrambling on easy energy landscapes, following the notion that in the McEliece cryptosystem the public and the private keys are connected through random permutations. We have shown in simplified settings that even if the energy landscape of the Hamiltonian induced by a private key has an easy-to-find ground state, then the energy-scrambling can introduce the phenomenon known as “clustering” into the energy landscape of the Hamiltonian induced by the public key. The clustering phenomenon is known for being an obstacle to local stochastic search algorithms.

In order to corroborate this picture, we studied numerically the performance of Parallel Tempering on Ising instances obtained from the McEliece protocol through our map – as an example of the stochastic local search approach – and the dedicated Stern algorithm crypto-attack on the original McEliece instances on the other. Indeed we observe much faster exponential TTS in the first case than for the second, confirming that in the absence of information about the structure of the underlying cryptographic problem, the scrambling map we developed produces hard to optimize Ising instances. These instances function as a filter for emerging combinatorial optimization accelerators that are *fundamentally* performing computation beyond local search.

VIII. CODE AVAILABILITY

Our implementations of the Stern algorithm and our parallel tempering solver for the McEliece instances are publicly available as part of the PySA Optimization Framework [70]. The code to generate random instances using the protocol presented in this paper is also available as part of PySA [71].

IX. ACKNOWLEDGMENTS

S.M, H.M.B, and G.M are KBR employees working under the Prime Contract No. 80ARC020D0010 with the NASA Ames Research Center. All the authors acknowledge funding from DARPA under NASA-DARPA SAA2-403688. We thank the NASA Advanced Supercomputing (NAS) division for resources on the Pleiades cluster. The United States Government retains, and by accepting the article for publication, the publisher acknowledges that the United States Government retains, a nonexclusive, paid-up, irrevocable, worldwide license to publish or reproduce the published form of this work, or allow others to do so, for United States Government purposes.

Appendix A: Typical Kernel Size For Random Matrices

The probability $\mathcal{P}(\alpha)$ of a given random matrix $\mathbf{S} \in \mathbb{F}_2^{k \times k}$ having a rank $\text{rank}(\mathbf{S}) = k - \alpha$ in the limit of $k \rightarrow \infty$ can be expressed as [72]:

$$\mathcal{P}(\alpha) = 2^{-\alpha^2} \frac{\prod_{j=\alpha+1}^{\infty} (1 - 2^{-j})}{\prod_{j=1}^{\alpha} (1 - 2^{-j})}, \quad (\text{A1})$$

where we used the convention that $\prod_{j=1}^0 (1 - 2^{-j}) = 1$. For instance, the probability of randomly sampling a non-singular matrix is then $\mathcal{P}(\alpha = 0) \approx 0.288788$. As shown in Fig. 4 and Table I, $\mathcal{P}(\alpha)$ quickly goes to zero:

TABLE I. Distribution of the rank of random matrices extracted from $\mathbb{F}_2^{k \times k}$, in the limit of $k \rightarrow \infty$.

Matrix Rank $[k - \alpha]$	$\mathcal{P}(\alpha)$
0	0.288788
1	0.577576
2	0.12835
3	$5.239 \cdot 10^{-3}$
4	$4.657 \cdot 10^{-5}$
5	$9.691 \cdot 10^{-8}$
6	$4.884 \cdot 10^{-11}$

with the number of elements in the kernel space having an average of $\langle 2^\alpha \rangle = 2$ and variance $\text{Var}[2^\alpha] = 1$.

Appendix B: Proof of the linear scrambling

In this appendix we will compute the probability

$$\Pr [E_x = \epsilon N, E_y = \epsilon N]$$

for the LSHWM to assign the energy value ϵN simultaneously to two states $x \neq y \in \{0, 1\}^N$, for $\epsilon > 0$. Clearly by linearity we have that if $\epsilon > 0$ and either of these states is the zero vector, then this probability must be zero. In

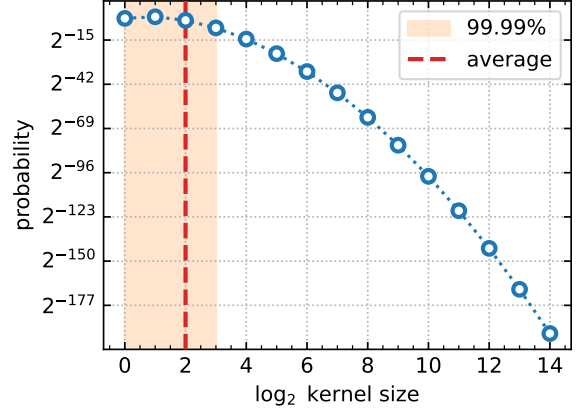


FIG. 4. Distribution of the size of the kernel of random matrices extracted from $\mathbb{F}_2^{k \times k}$, in the limit of $k \rightarrow \infty$. The shaded area corresponds to the 99.99% of the distribution, while the dashed line corresponds to its average.

the following we will assume that neither x nor y are zero. Given a realization of disorder $\mathbf{S} = \{a_{ij}\}$ (*i.e.* a random matrix of the LSHWM ensemble), the energies of x, y are

$$E_x = \sum_{j=1}^N \left[\sum_{k=1}^N a_{jk} x_k \pmod{2} \right] \equiv \sum_{j=1}^N E_x^{(j)},$$

$$E_y = \sum_{j=1}^N \left[\sum_{k=1}^N a_{jk} y_k \pmod{2} \right] \equiv \sum_{j=1}^N E_y^{(j)}.$$

We partition the set $[N] \equiv \{1, 2, \dots, N\}$ as

$$[N] = \{k \mid x_k = y_k = 0\} \cup \{k \mid x_k = y_k = 1\} \\ \cup \{k \mid x_k = 0, y_k = 1\} \cup \{k \mid x_k = 1, y_k = 0\} \\ \equiv (00) \cup (11) \cup (01) \cup (10)$$

and coarse-grain the disordered degrees of freedoms $\{a_{jk}\}$ in $2^{\alpha N}$ “macrostates” $\mathcal{S} \in \{0, 1\}^{\alpha N}$ where each of the αN coarse-grained binary variables $\mathcal{S}_\gamma^{(j)}$ of \mathcal{S} are functions of the matrix entries $\{a_{jk}\}_{jk}$. For each $j = 1, \dots, N$ we define

$$\mathcal{S}_\gamma^{(j)} \equiv \sum_{k \in \gamma} a_{jk} \pmod{2}, \quad \text{for } \gamma \in \{(00), (01), (10), (11)\}$$

so that

$$\mathcal{S} = \left(\left\{ \mathcal{S}_{00}^{(j)} \right\}_{j=1}^N, \left\{ \mathcal{S}_{01}^{(j)} \right\}_{j=1}^N, \left\{ \mathcal{S}_{10}^{(j)} \right\}_{j=1}^N, \left\{ \mathcal{S}_{11}^{(j)} \right\}_{j=1}^N \right).$$

The integer $\alpha \in \{2, 3, 4\}$ will depend on the states x, y (specifically, whether or not there exist indices k where $x_k = y_k = 0$ so that the set (00) is nonempty, and analogously for (01), (10) and (11)), and we will distinguish cases. A specific choice of values for the disordered variables $\{a_{jk}\}_{jk}$ will induce a unique macrostate, *i.e.* an assignment of Boolean values to all variables $\{\mathcal{S}_\gamma^{(j)}\}_{j,\gamma}$,

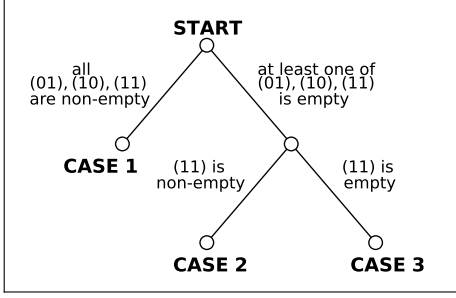


FIG. 5. Logical flowchart of the three main cases for the calculation of the probability $\Pr[E_x = \epsilon N, E_y = \epsilon N]$ in the LSHWM.

while a specific choice of values for $\{\mathcal{S}_\gamma^{(j)}\}_{j,\gamma}$ will be compatible with multiple “microstates” $\{a_{jk}\}_{jk}$. Note that the variables a_{ij} involved in the definitions of the $\mathcal{S}_\gamma^{(j)}$ for different γ , are all independent.

Then the energies of the states x, y we can be written as a function of the macrostate variables:

$$E_x = \sum_{j=1}^N E_x^{(j)} = \sum_{j=1}^N \left[\mathcal{S}_{11}^{(j)} + \mathcal{S}_{10}^{(j)} \pmod{2} \right]$$

$$E_y = \sum_{j=1}^N E_y^{(j)} = \sum_{j=1}^N \left[\mathcal{S}_{11}^{(j)} + \mathcal{S}_{01}^{(j)} \pmod{2} \right]$$

Observe in particular that the energies do not depend on the macrostate variables $\mathcal{S}_{00}^{(j)}$. In order to compute the probability of having $E_x = E_y = \epsilon N$ we need to count how many ways we can choose values for the macrostate variables that will give us this energy value for both E_x and E_y , and then weight each choice by its appropriate probability induced by the distribution of the microscopic degrees of freedom $\{a_{jk}\}_{jk}$ compatible with that choice. We distinguish the following three main cases, summarized in Fig. 5.

- **Case 1: the three subsets $\gamma = (11), (01), (10)$ are non-empty.** Let us fix a vector $\mathcal{S}_{11} = (\mathcal{S}_{11}^{(1)}, \dots, \mathcal{S}_{11}^{(N)}) \in \{0, 1\}^N$. In order to have $E_x = \epsilon N$ we need to have ϵN indices $0 \leq j \leq N$ where $E_x^{(j)} = 1$. This fixes the values of $\mathcal{S}_{10}^{(j)}$ since we need to have ϵN indices where $\mathcal{S}_{10}^{(j)} = 1 - \mathcal{S}_{11}^{(j)}$ and the other $(1 - \epsilon)N$ must be $\mathcal{S}_{11}^{(j)} = \mathcal{S}_{10}^{(j)}$. Analogously we need to choose ϵN values of j where $E_y^{(j)} = 1$. These can be chosen independently from the choices of $E_x^{(j)}$. This fixes the values $\mathcal{S}_{01}^{(j)}$.
- **Case 1.A: the subset (00) is non-empty**
Then $\alpha = 4$ and we have the N degrees of freedom in $\mathcal{S}_{00}^{(j)}$ that are completely free and

do not affect the energies at all. So for a fixed $\mathcal{S}_{11} = (\mathcal{S}_{11}^{(1)}, \dots, \mathcal{S}_{11}^{(N)}) \in \{0, 1\}^N$ we have

$$2^N \binom{N}{\epsilon N}^2$$

choices to achieve that $E_x = E_y = \epsilon N$. Which means that at the level of the macrostates \mathcal{S} , the number n_M of choices that give $E_x = E_y = \epsilon N$ is

$$n_M = 2^{2N} \binom{N}{\epsilon N}^2$$

What is left to do is to compute the entropies of the macrostates. A given value $\mathcal{S}_\gamma^{(j)}$ is compatible with half of the microstates of the variables a_{ij} that appear in its definition, and all of these choices are independent for different j and γ , so we get (remember that here $\alpha = 4$)

$$2^{-\alpha N} \left[2^N \right]^N 2^{2N} \binom{N}{\epsilon N}^2 = 2^{N^2} 2^{-2N} \binom{N}{\epsilon N}^2$$

out of a total of 2^{2N} microstates, so the probability we seek is given by

$$\Pr[E_\sigma = \epsilon N, E_\tau = \epsilon N] = 2^{-2N} \binom{N}{\epsilon N}^2 \equiv P_\epsilon$$

- **Case 1.B: the subset (00) is empty** In this case $\alpha = 3$ and we have already fixed all macrostate variables. By an analogous calculation to the Case 1.A we have

$$n_M = 2^N \binom{N}{\epsilon N}^2$$

choices for the macrostate variables compatible with $E_x = E_y = \epsilon N$. In the language of the microstates, we have

$$2^{-\alpha N} \left[2^N \right]^N 2^N \binom{N}{\epsilon N}^2 = 2^{N^2} 2^{-2N} \binom{N}{\epsilon N}^2$$

choices out of 2^{2N} total microstates. This gives the same value P_ϵ for the probability, as before.

- **Case 2: (11) is non-empty, and at least one between (01), (10) is empty.** Notice that in this case we must have that *exactly* one between (01), (10) is empty (if both are empty then $x = y$, a possibility that we have ruled out by assumption). Since the states x, y play a perfectly symmetrical role in the probability we are trying to compute we can assume without loss of generality that (01) is non-empty and (10) is empty. In this case, in order to have $E_x = \epsilon N$ we have to choose ϵN variables

$\mathcal{S}_{11}^{(j)}$ to be set to one, and all the others to zero ($\binom{N}{\epsilon N}$ choices). This fixes the vector \mathcal{S}_{11} . In order to obtain $E_y = \epsilon N$ we have to choose ϵN variables $\mathcal{S}_{01}^{(j)}$ to be set equal to $\mathcal{S}_{01}^{(j)} = 1 - \mathcal{S}_{11}^{(j)}$ and the others to $\mathcal{S}_{01}^{(j)} = \mathcal{S}_{11}^{(j)}$ (another $\binom{N}{\epsilon N}$ choices). This fixes the vector \mathcal{S}_{01} .

– **Case 2.A: the subset (00) is non-empty**
Then $\alpha = 3$ and the proof follows Case 1.A with $n_M = 2^N \binom{N}{\epsilon N}$ which leads to a probability of P_ϵ as before.

– **Case 2.B: the subset (00) is empty** Then $\alpha = 2$ and the proof follows Case 2.A with $n_M = \binom{N}{\epsilon N}$ which leads to a probability of P_ϵ as before.

- **Case 3: (11) is empty.** In this case we must have that both (01) and (10) are non-empty, otherwise at least one between x and y is the zero vector, a possibility that we have ruled out by assumption. In order to have $E_x = E_y = \epsilon N$ we have to set to one exactly ϵN variables $\mathcal{S}_{01}^{(j)}$, and exactly ϵN variables $\mathcal{S}_{10}^{(j)}$, independently. This gives $\binom{N}{\epsilon N}^2$ choices. This fixes the vectors \mathcal{S}_{01} and \mathcal{S}_{10} .

– **Case 3.A: the subset (11) is non-empty**
Then $\alpha = 3$ and the proof follows Case 1.A with $n_M = 2^N \binom{N}{\epsilon N}$ which leads to a probability of P_ϵ as before.

– **Case 3.B: the subset (11) is empty** Then $\alpha = 2$ and the proof follows Case 2.A with $n_M = \binom{N}{\epsilon N}$ which leads to a probability of P_ϵ as before.

Appendix C: Computational Algorithms

Stern’s Algorithm. Let us give a detailed overview of the information set decoding (ISD) strategy. Given a binary matrix $H \in \mathbb{F}_2^{(N-k) \times n}$ and a vector $y \in \mathbb{F}_2^{(N-k)}$, Stern’s algorithm searches for a vector $x \in \mathbb{F}_2^n$ of Hamming weight $\|x\| \leq t$ such that

$$Hx \equiv y \pmod{2}. \quad (\text{C1})$$

Alternatively, given a binary matrix $H \in \mathbb{F}_2^{(N-k) \times n}$, search for a non-zero vector $x \in \mathbb{F}_2^n$ of minimum Hamming weight such that

$$Hx \equiv 0 \pmod{2}. \quad (\text{C2})$$

The steps involved in information decoding are as follows:

1. (Initialization) Initialize the augmented matrix

$$A \equiv (H|y) \quad (\text{C3})$$

where the N columns of H are the “principal” columns and the additional column y is the sole

augmented column. If calculating code distance, then we simply have $y = 0$, so augmentation is not necessary.

Algorithm 1. Stern’s Algorithm, “heavy” version. The subroutine GJE(A, R) performs Gauss-Jordan elimination on the matrix A using the list of columns R as pivots.

```

1: procedure STERN( $H \in \mathbb{F}_2^{(N-k) \times n}, y \in \mathbb{F}_2^{(N-k)}$ )
2:   Initialize  $A \leftarrow (H|y)$ , which has  $N$  principal columns
   and  $y$  is the sole augmented column.
3:   repeat
4:     Randomly sample an IR partition  $(I, R)$  of the
   principal columns of  $A$ .
5:      $A' = (H'|y') \leftarrow \text{GJE}(A, R)$ 
6:     until  $A'_{|R}$  is full rank.
7:     Randomly split  $I$  into  $I_1$  and  $I_2$ .
8:     for Each combination  $(i_1, \dots, i_p)$  from  $I_1$  do
9:       for Each combination  $(j_1, \dots, j_p)$  from  $I_2$  do
10:        Let  $b \leftarrow \sum_n A'_{i_n} + \sum_m A'_{j_m} + y'$ 
11:        if  $\text{HW}(b) = t - 2p$  then
12:           $\mathcal{E} \leftarrow \{k | b_k > 0\} \cup \{i_1, \dots, i_p\} \cup \{j_1, \dots, j_p\}$ 
13:          Return the error set  $\mathcal{E}$ 
14:        end if
15:      end for
16:    end for
17:    Return failure.
18: end procedure

```

augmented column. If calculating code distance, then we simply have $y = 0$, so augmentation is not necessary.

2. (IR Partition) Randomly partition the N principal columns of A into an information/redundancy set pair (I, R) . Perform binary Gauss-Jordan elimination on A over the columns indexed by R , restarting with a new random pair if the submatrix $A_{|R}$ is not full rank. Denote by y' the final column of A after elimination.
3. (Combinatorial Search) Search for vectors $x_0 \in \mathbb{F}_2^{N-k}$ and $x_1 \in \mathbb{F}_2^k$ such that the objective

$$\mathcal{L}(x_0, x_1) = \|y' - (x_0 + A_{|I}x_1)\|, \quad (\text{C4})$$

is minimized to 0 subject to the constraint $\|x_0\| + \|x_1\| \leq t$. If calculating the code distance, then perform the minimization subject to the constraint that $\|x_0\| > 0$. The solution x is gathered from x_0 and x_1 so that $x_{|R} = x_0$ and $x_{|I} = x_1$.

4. (Result) If minimization succeeds, return the solution x . Otherwise, return to step 2 until termination/time-out.

Stern’s algorithm is an implementation of ISD where the combinatorial search step randomly splits the information set I into two sets, I_1 and I_2 then searches for a linear combination consisting of y' with p columns from I_1 and p columns from I_2 that has a Hamming weight of exactly $w - 2p$. If such a combination is found, the indices of the non-zero bits are precisely the error bits in the redundancy set, and the $2p$ columns are the remaining error bits contained in the information set. The

TABLE II. Table of parameters used for parallel tempering.

N_T	β_{\min}	β_{\max}	N_{Steps}
16	0.1	1.0	10^7

specific procedure is shown in Algorithm 1. Our implementation is a “heavy” version of Stern’s algorithm that skips collision checking on the $2p$ columns before calculating the full Hamming weight. The collision check was observed to have a negative impact for all parameter sets in our benchmarks. The p integer parameter (unrelated to p as in p -local Hamiltonian) of Stern’s algorithm was fixed to $p = 1$, as larger values did not benefit the theoretical success probability for the parameter sets used here.

When mapped to a corresponding p -local Hamiltonian, the IR partition defines a gauge transformation on the spin variables such that $N - k$ terms are reduced to linear interactions. This transformation simplifies the chosen terms in the Hamiltonian in exchange for potentially higher-order interactions on the remaining terms. ISD is therefore well-suited for an unstructured p -local Hamiltonian where p is already large and there is no clear interaction locality. On the other hand, if p is small, local search heuristics may be more effective, while ISD unnecessarily transforms the problem to include higher-order interactions.

Parallel Tempering. The parallel tempering algorithm, also known as replica exchange Monte Carlo, is a Markov Chain Monte Carlo algorithm that performs Metropolis-Hastings sampling on multiple replicas at different temperatures [64–66]. The replicas converge to thermal equilibrium by including a move to swap two replicas in neighboring temperatures and occasionally performing this move under the Metropolis-Hastings criterion. This accelerates the convergence of low-temperature states of Ising spin glasses compared to sampling at a single temperature alone. A variation of PT that performs energy-conserving (“isoenergetic”) cluster moves across replicas (called PT-ICM) has been especially successful in benchmarks against quantum annealing for finding the ground-state energy of finite-dimensional Ising spin glasses [6, 34, 35]. As the instances we generate are dense, rather than finite-dimensional, there is no computational advantage in performing cluster moves, so we only benchmark the ordinary PT algorithm rather than PT-ICM. The procedure of our implementation is given in Algorithm 2.

We used a geometrically spaced array of inverse temperatures, *i.e.* $\beta_i = e^{x\beta_{\min} + (1-x_i)\beta_{\max}}$ where $x_i = (N_T - i)/(N_T - 1)$ where $i = 1, 2, \dots, N_T$ is the index of each replica temperature, β_{\min} is the smallest inverse temperature, and β_{\max} is the largest inverse temperature. We chose N_T , β_{\min} and β_{\max} so that the time-to-solution for a few instances at $k = 16$ through 20 was satisfactory across individual runs on a personal computer and the number of accepted replica exchange moves was not

Algorithm 2. Parallel tempering algorithm for a p -local Ising Hamiltonian. $\text{Rand}()$ is a call to a uniformly random floating point number in the interval $[0, 1)$.

```

1: procedure PT(Hamiltonian  $H(\sigma)$  for an  $[N, k, t]$  code,
    $N_T, \beta_i, N_{\text{steps}}$ )
2:   Randomly initialize replicas  $\sigma^{(i)}, i = 1, \dots, N_T$  .
3:   for  $t \in 1, \dots, N_{\text{steps}}$  do
4:     for  $i \in \{1, \dots, N_T\}$  do
5:       for  $j \in 1, \dots, k$  do ▷ Sweep replica  $i$ 
6:         Calculate  $\Delta E$  of flipping spin  $j$  in  $H(\sigma_i)$ 
7:          $p \leftarrow e^{-\beta \Delta E}$ 
8:         if  $\Delta E < 0$  or  $\text{Rand}() < p$  then
9:            $\sigma_j^{(i)} \leftarrow -\sigma_j^{(i)}$ 
10:        end if
11:        if  $H(\sigma^{(i)}) = t - N$  then
12:           $x_j \leftarrow (1 - \sigma_j^{(i)})/2$ 
13:          Return decoded message  $x$ .
14:        end if
15:      end for
16:    end for
17:    for  $i \in \{1, \dots, N_T - 1\}$  do ▷ Replica exchange
   moves
18:       $f \leftarrow (\beta_{i+1} - \beta_i)(E_{i+1} - E_i)$ 
19:      if  $f \geq 0$  or  $\text{Rand}() < e^f$  then
20:        Swap replicas  $i$  and  $i + 1$ 
21:      end if
22:    end for
23:  end for
24:  Return failure.
25: end procedure

```

depressed at any temperature. We did not attempt additional optimization of the array of temperatures. Because the scrambled energy landscape thwarts any algorithm relying on local moves, it is unlikely that the scaling is sensitive to any further optimization of the PT parameters. The parameters of our PT benchmarks are fully specified in Table II.

Appendix D: Generation of McEliece Instances

We used random Goppa codes as the underlying code for the McEliece protocol, but allowed the ability to tune all code parameters to generate computationally tractable benchmarking instances to perform our scaling analysis. We implemented a random instance generator with the McEliece cryptographic protocol which takes the desired code length N and error correcting distance t as inputs, as well as an additional parameter $m \geq \lceil \log_2 N \rceil$ for the Goppa code. The message length is determined as $k = N - tm$. Instance generation is performed in following steps:

1. Generate a random k -bit plain-text message q to encode and a random weight t error ϵ .
2. Generate a random irreducible degree t polynomial P over \mathbb{F}_{2^m} . This can be done by rejection sampling on random polynomials over \mathbb{F}_{2^m} . The ex-

pected number of trials of rejection sampling before finding an irreducible polynomial is no greater than the degree of the polynomial, *i.e.* $O(t)$, while the average cost of testing for irreducibility via Rabin's algorithm is $O(mt^2)$ (the polynomial degree times the cost of polynomial multiplication) [73]. Thus, the average case complexity of generating a random irreducible polynomial is $O(mt^3)$.

3. Generate a random Goppa code by randomly sampling N elements α_i from the finite field \mathbb{F}_{2^m} . The generator matrix \mathbf{G} and error correcting algorithm are defined using the value of P evaluated on each of the N elements (see, *e.g.*, [46, 74]). For consistency with the desired message length, the Goppa code is rejected and re-sampled from step 2 if the null space of \mathbf{G} is larger than k .
4. Randomly generate \mathbf{S} and \mathbf{P} to construct the public key \mathbf{G}' from \mathbf{G} .

5. Encrypt the message via Eq. (7).

Thus, we have the \mathbf{G}' and q' which completely define the McEliece problem instance and hence the scrambled Ising Hamiltonian. The instance is solved if the plain-text message q (or equivalently the error vector ϵ) is found.

While we have made every effort to test the correctness of the generator, encoder, and decoder, our aim was to generate cryptographic problems with tunable attack complexity and thus made no attempt at ensuring compliance with the Classic McEliece specifications. One important difference is that our time-complexity to generate a public/private key pair is dominated by the second step—finding a random irreducible polynomial over \mathbb{F}_{2^m} as $O(mt^3)$. The Classic McEliece specification does not use Rabin's algorithm for the secure generation of a random irreducible polynomial since its success rate decreases with the desired security of the public/private key pair.

-
- [1] F. Arute, K. Arya, R. Babbush, D. Bacon, J. C. Bardin, R. Barends, R. Biswas, S. Boixo, F. G. Brandao, D. A. Buell, *et al.*, *Nature* **574**, 505 (2019).
 - [2] A. Morvan, B. Villalonga, X. Mi, S. Mandrà, A. Bengtsson, P. Klimov, Z. Chen, S. Hong, C. Erickson, I. Drozdov, *et al.*, *Nature* **634**, 328 (2024).
 - [3] Y. Kim, A. Eddins, S. Anand, K. X. Wei, E. Van Den Berg, S. Rosenblatt, H. Nayfeh, Y. Wu, M. Zaletel, K. Temme, *et al.*, *Nature* **618**, 500 (2023).
 - [4] M. Kim, S. Mandrà, D. Venturelli, and K. Jamieson, in *Proceedings of the 27th Annual International Conference on Mobile Computing and Networking* (2021) pp. 42–55.
 - [5] M. Aramon, G. Rosenberg, E. Valiante, T. Miyazawa, H. Tamura, and H. G. Katzgraber, *Frontiers in Physics* **7**, 48 (2019).
 - [6] Z. Zhu, A. J. Ochoa, and H. G. Katzgraber, *Physical Review Letters* **115**, 077201 (2015).
 - [7] N. Mohseni, P. L. McMahon, and T. Byrnes, *Nature Reviews Physics* **4**, 363 (2022).
 - [8] M. Sao, H. Watanabe, Y. Musha, and A. Utsunomiya, *Fujitsu Scientific and Technical Journal* **55**, 45 (2019).
 - [9] F. L. Traversa and M. Di Ventra, *IEEE Transactions on Neural Networks and Learning Systems* **26**, 2702 (2015).
 - [10] L. M. Adleman, *Science* **266**, 1021 (1994).
 - [11] C. H. Papadimitriou and K. Steiglitz, *Combinatorial optimization: algorithms and complexity* (Courier Corporation, 1998).
 - [12] M. Sipser, *ACM Sigact News* **27**, 27 (1996).
 - [13] A. Biere, M. Heule, and H. van Maaren, *Handbook of satisfiability*, Vol. 185 (IOS press, 2009).
 - [14] G. Qu and M. Potkonjak, in *International Workshop on Information Hiding* (Springer, 1999) pp. 348–367.
 - [15] W. Barthel, A. K. Hartmann, M. Leone, F. Ricci-Tersenghi, M. Weigt, and R. Zecchina, *Physical Review Letters* **88**, 188701 (2002).
 - [16] F. Krzakala and L. Zdeborová, *Physical Review Letters* **102**, 238701 (2009).
 - [17] L. Zdeborová and F. Krzakala, *SIAM Journal on Discrete Mathematics* **25**, 750 (2011).
 - [18] F. Krzakala, M. Mézard, and L. Zdeborová, *Journal on Satisfiability, Boolean Modeling and Computation* **8**, 149 (2012).
 - [19] G. Sicuro and L. Zdeborová, *Journal of Physics A: Mathematical and Theoretical* **54**, 175002 (2021).
 - [20] M. Mézard, G. Parisi, and R. Zecchina, *Science* **297**, 812 (2002).
 - [21] L. Zdeborová and F. Krzakala, *Physical Review E* **76**, 031131 (2007).
 - [22] F. Ricci-Tersenghi, G. Semerjian, and L. Zdeborová, *Physical Review E* **99**, 042109 (2019).
 - [23] G. Semerjian, G. Sicuro, and L. Zdeborová, *Physical Review E* **102**, 022304 (2020).
 - [24] L. Zdeborová and M. Mézard, *Journal of Statistical Mechanics: Theory and Experiment* **2008**, P12004 (2008).
 - [25] V. S. Denchev, S. Boixo, S. V. Isakov, N. Ding, R. Babbush, V. Smelyanskiy, J. Martinis, and H. Neven, *Physical Review X* **6**, 031015 (2016).
 - [26] I. Hen, J. Job, T. Albash, T. F. Rønnow, M. Troyer, and D. A. Lidar, *Physical Review A* **92**, 042325 (2015).
 - [27] W. Wang, S. Mandrà, and H. G. Katzgraber, *Physical Review E* **96**, 023312 (2017).
 - [28] F. Hamze, D. C. Jacob, A. J. Ochoa, D. Perera, W. Wang, and H. G. Katzgraber, *Physical Review E* **97**, 043303 (2018).
 - [29] D. Perera, F. Hamze, J. Raymond, M. Weigel, and H. G. Katzgraber, *Physical Review E* **101**, 023316 (2020).
 - [30] I. Hen, *Physical Review Applied* **12**, 011003 (2019).
 - [31] F. Hamze, J. Raymond, C. A. Pattison, K. Biswas, and H. G. Katzgraber, *Physical Review E* **101**, 052102 (2020).
 - [32] D. J. Thouless, P. W. Anderson, and R. G. Palmer, *Philosophical Magazine* **35**, 593 (1977).
 - [33] J. King, S. Yarkoni, J. Raymond, I. Ozfidan, A. D. King, M. M. Nevisi, J. P. Hilton, and C. C. McGeoch, *Journal of the Physical Society of Japan* **88**, 061007 (2019).
 - [34] S. Mandrà, Z. Zhu, W. Wang, A. Perdomo-Ortiz, and H. G. Katzgraber, *Physical Review A* **94**, 022337 (2016).

- [35] S. Mandrà, H. G. Katzgraber, and C. Thomas, *Quantum Science and Technology* **2**, 038501 (2017).
- [36] S. Mandrà, B. Villalonga, S. Boixo, H. Katzgraber, and E. Rieffel, in *APS March Meeting Abstracts*, Vol. 2019 (2019) pp. C42–013.
- [37] S. Mandrà and H. G. Katzgraber, *Quantum Science and Technology* **3**, 04LT01 (2018).
- [38] J. Marshall, V. Martin-Mayor, and I. Hen, *Physical Review A* **94**, 012320 (2016).
- [39] R. Merkle and M. Hellman, *IEEE Transactions on Information Theory* **24**, 525 (1978).
- [40] C. H. Papadimitriou, in *Encyclopedia of computer science* (2003) pp. 260–265.
- [41] A. Shamir, in *23rd Annual Symposium on Foundations of Computer Science (sfcs 1982)* (IEEE, 1982) pp. 145–152.
- [42] N. Pirnay, V. Ulitzsch, F. Wilde, J. Eisert, and J.-P. Seifert, *Science Advances* **10**, eadj5170 (2024).
- [43] M. Szegeedy, arXiv:2212.12572 (2022).
- [44] P. W. Shor, *SIAM Review* **41**, 303 (1999).
- [45] R. J. McEliece, *Coding Thv* **4244**, 114 (1978).
- [46] D. J. Bernstein, T. Lange, and C. Peters, in *Post-Quantum Cryptography: Second International Workshop, PQCrypto 2008 Cincinnati, OH, USA, October 17-19, 2008 Proceedings 2* (Springer, 2008) pp. 31–46.
- [47] H. Dinh, C. Moore, and A. Russell, in *Advances in Cryptology–CRYPTO 2011: 31st Annual Cryptology Conference, Santa Barbara, CA, USA, August 14-18, 2011. Proceedings 31* (Springer, 2011) pp. 761–779.
- [48] NIST, Post-quantum cryptography (PQC), <https://csrc.nist.gov/projects/post-quantum-cryptography/round-3-submissions>.
- [49] N. Surlas, *Nature* **339**, 693 (1989).
- [50] H. Nishimori, *Statistical Physics of Spin Glasses and Information Processing: An Introduction* (Oxford University Press, 2001).
- [51] M. Mézard, T. Mora, and R. Zecchina, *Physical Review Letters* **94**, 197205 (2005).
- [52] D. Achlioptas and F. Ricci-Tersenghi, in *Proceedings of the Thirty-Eighth Annual ACM Symposium on Theory of Computing*, STOC '06 (Association for Computing Machinery, New York, NY, USA, 2006) p. 130–139.
- [53] A. Coja-Oghlan, A. Haqshenas, and S. Hetterich, *SIAM Journal on Discrete Mathematics* **31**, 1160 (2017), <https://doi.org/10.1137/16M1084158>.
- [54] D. Gamarnik, *Proceedings of the National Academy of Sciences* **118**, e2108492118 (2021), <https://www.pnas.org/doi/pdf/10.1073/pnas.2108492118>.
- [55] M. C. Angelini and F. Ricci-Tersenghi, *Physical Review X* **13**, 021011 (2023).
- [56] By changing into the binary representation $X = (x_1, \dots, x_N) \in \{0, 1\}^N$ of the spin configuration σ through the defining $x_i = (1 - \sigma_i)/2$, then $H(\sigma)$ is the Hamming weight of the associated binary string X .
- [57] E. Farhi, J. Goldstone, D. Gosset, S. Gutmann, and P. W. Shor, *Quantum Information and Computation* **11**, 840 (2011).
- [58] This is observed also in *e.g.* the Random Energy Model, where $\Phi_{x,\epsilon} = \ln(2) + S(x) - 2\epsilon^2$.
- [59] L. Zdeborová and F. Krzakala, *Physical Review E* **76**, 031131 (2007).
- [60] G. Semerjian, *Journal of Statistical Physics* **130**, 251 (2008).
- [61] A. Becker, A. Joux, A. May, and A. Meurer, in *Advances in Cryptology – EUROCRYPT 2012*, Lecture Notes in Computer Science, edited by D. Pointcheval and T. Johansson (Springer, Berlin, Heidelberg, 2012) pp. 520–536.
- [62] J. Stern, in *Coding Theory and Applications*, Lecture Notes in Computer Science, edited by G. Cohen and J. Wolfmann (Springer, Berlin, Heidelberg, 1989) pp. 106–113.
- [63] A. Canteaut and F. Chabaud, *IEEE Transactions on Information Theory* **44**, 367 (1998).
- [64] R. H. Swendsen and J.-S. Wang, *Physical review letters* **57**, 2607 (1986).
- [65] E. Marinari and G. Parisi, *Europhysics letters* **19**, 451 (1992).
- [66] K. Hukushima and K. Nemoto, *Journal of the Physical Society of Japan* **65**, 1604 (1996).
- [67] D. J. Bernstein and T. Chou, *CryptAttackTester: High-assurance attack analysis* (2023).
- [68] D. J. Bernstein, in *Post-Quantum Cryptography*, Vol. 6061, edited by D. Hutchison, T. Kanade, J. Kittler, J. M. Kleinberg, F. Mattern, J. C. Mitchell, M. Naor, O. Nierstrasz, C. Pandu Rangan, B. Steffen, M. Sudan, D. Terzopoulos, D. Tygar, M. Y. Vardi, G. Weikum, and N. Sendrier (Springer Berlin Heidelberg, Berlin, Heidelberg, 2010) pp. 73–80.
- [69] S. Wang, E. Fontana, M. Cerezo, K. Sharma, A. Sone, L. Cincio, and P. J. Coles, *Nature Communications* **12**, 6961 (2021).
- [70] PySA: Stern Algorithm Solver, <https://github.com/nasa/PySA/tree/pysa-stern> (2024).
- [71] PySA: McEliece Instance Generator, <https://github.com/nasa/PySA/tree/pysa-mceliece> (2024).
- [72] C. Cooper, *Random Structures & Algorithms* **17**, 197 (2000).
- [73] D. Panario and A. Viola, in *LATIN'98: Theoretical Informatics*, edited by C. L. Lucchesi and A. V. Moura (Springer, Berlin, Heidelberg, 1998) pp. 1–10.
- [74] N. Patterson, *IEEE Transactions on Information Theory* **21**, 203 (1975).